Science

AAAS

The Ste5 Scaffold Allosterically Modulates Signaling Output of the Yeast Mating Pathway

Roby P. Bhattacharyya,[1,2]* Attila Reményi,[1]* Matthew C. Good,[1,2] Caleb J. Bashor,[1,3] Arnold M. Falick,[4] Wendell A. Lim[1]†

Scaffold proteins organize signaling proteins into pathways and are often viewed as passive assembly platforms. We found that the Ste5 scaffold has a more active role in the yeast mating pathway: A fragment of Ste5 allosterically activated autophosphorylation of the mitogen-activated protein kinase Fus3. The resulting form of Fus3 is partially active—it is phosphorylated on only one of two key residues in the activation loop. Unexpectedly, at a systems level, autoactivated Fus3 appears to have a negative regulatory role, promoting Ste5 phosphorylation and a decrease in pathway transcriptional output. Thus, scaffolds not only direct basic pathway connectivity but can precisely tune quantitative pathway input-output properties.

Cells use networks of intracellular signaling proteins to detect and process environmental stimuli and to make complex response decisions. A central question in cell biology is how such signals are accurately and specifically transmitted through these pathways, especially given the vast number of similar signaling proteins that exist in a given cell. In many cases, scaffold proteins—proteins that bind and organize multiple proteins within a pathway—have emerged as important factors in mediating signaling efficiency and specificity (1, 2). By tethering components together, scaffolds are thought to promote interaction of the proper partners and to prevent signaling to improper partners. The scaffold protein Ste5 is required for signaling through the mating (or pheromone) response mitogen-activated protein kinase (MAPK) pathway in *Saccharomyces cerevisiae* (3). Ste5 has separable binding sites for each member of the mating MAPK cascade: the MAPK Fus3, the MAPK kinase (MAPKK) Ste7, and the MAPKK kinase (MAPKKK) Ste11 (4–6). A scaffold is thought to be particularly important for directing signals through the mating pathway, because several functionally distinct MAPK cascades in yeast use an overlapping set of kinase components (e.g., Ste11 is also a member of the osmo-response and filamentation pathways, and Ste7 is also a member of the filamentation pathway) (7, 8).

Despite the importance of Ste5 as a prototypical scaffold, little is known about the structural and molecular basis for its function (1, 9, 10). How does it interact with the kinases and how does it promote proper signaling? Here, we focus on understanding how the mating MAPK, Fus3, is recruited to the Ste5 complex. We mapped the interaction sites, determined the structural basis of the interactions, and analyzed how they contribute to pathway signaling in vivo. We uncovered several unexpected findings: Within the Ste5 complex, multiple independent recruitment sites for Fus3 contribute to pathway function; some of these sites do not function as passive tethering sites but rather can allosterically activate the kinase; and these sites can precisely modulate pathway output, not only by promoting signal propagation but also by mediating phosphorylation events that limit pathway output.

Mapping Fus3 binding sites. The MAPK Fus3 physically interacts with two members of the mating pathway, the scaffold Ste5 and the upstream MAPKK Ste7 (Fig. 1A). Fus3 interacts with Ste7 through a canonical MAPK docking interaction; Ste7 contains a motif matching the consensus sequence $(R/K)_{1,2}x_{3-8}LxL$ (one or two Arg or Lys in the first positions, a spacer region three to eight amino acids in length, and two Leu residues separated by one amino acid) (11, 12). Such docking motifs are found in diverse MAPK binding partners and bind to a groove on the surface directly opposite the kinase active site (13–15). Previous studies have suggested that the docking motif in Ste7 makes a marginal contribution to mating pathway function (12). However, we have recently found that Ste7 contains a second MAPK docking motif, also near the N terminus (16) (Fig. 1B), and we present a functional analysis of both motifs here. We have also solved the structure of one of the Ste7 docking peptides bound to Fus3 (16).

In contrast, little is known about the interaction of Fus3 with Ste5. This interaction was first mapped by yeast two-hybrid analysis to a 96–amino acid stretch in Ste5 (4). We refined this binding region through a series of deletion constructs to a minimal ∼30-residue polypeptide [residues 288 to 316 (Ste5_pep)] that is sufficient for binding (Fig. 1B and fig. S1). This polypeptide shows no apparent similarity to other MAPK docking motifs, including the docking peptides in Ste7. Using fluorescence polarization, we have measured the dissociation constant (K_d) of this Ste5 fragment for Fus3 to be 4 μM (fig. S2), which is comparable to the affinities of the docking peptides from Ste7 ($K_d^{Ste7\_pep1} = 0.08$ μM; $K_d^{Ste7\_pep2} = 12$ μM) (16).

Structure of Fus3-Ste5 complex and comparison to canonical MAPK docking interactions. We solved the crystal structure of the Ste5 fragment in complex with Fus3 (Fig. 2) (17). This complex is unlike others observed for MAPKs. The Ste5 fragment binds Fus3 in a bipartite manner, extending over the entire backside of the kinase to contact
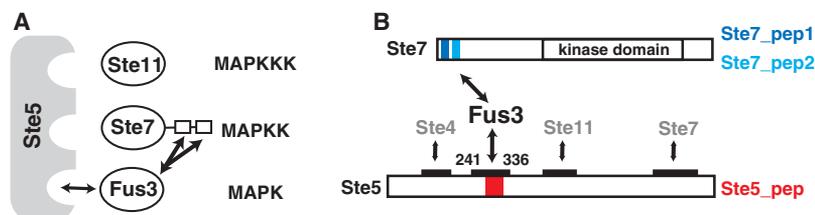
[1]Department of Cellular and Molecular Pharmacology, [2]Program in Biological Sciences, [3]Graduate Group in Biophysics, University of California–San Francisco, 600 16th Street, San Francisco, CA 94143–2240, USA. [4]Howard Hughes Medical Institute Mass Spectrometry Laboratory, University of California–Berkeley, 17 Barker Hall, Berkeley, CA 94720, USA.

*These authors contributed equally to this work.
†To whom correspondence should be addressed. E-mail: lim@cmp.ucsf.edu

Fig. 1. Fus3 recruitment to the pheromone response MAPK complex. (**A**) Schematic of pheromone response MAPK complex. The MAPK Fus3 interacts with the scaffold protein Ste5 (4–6) and the MAPKK Ste7 (6, 40). (**B**) Maps of the interaction domains in the MAPKK Ste7 and the scaffold Ste5. Minimal Fus3 binding peptides are shown in color [dark blue, Ste7_pep1 (12, 16); light blue, Ste7_pep2 (16)]. Black bars above the Ste5 schematic indicate protein-interaction domains identified in yeast two-hybrid assays (4, 37). The Fus3 binding peptide (Ste5_pep) is shown in red (fig. S1).
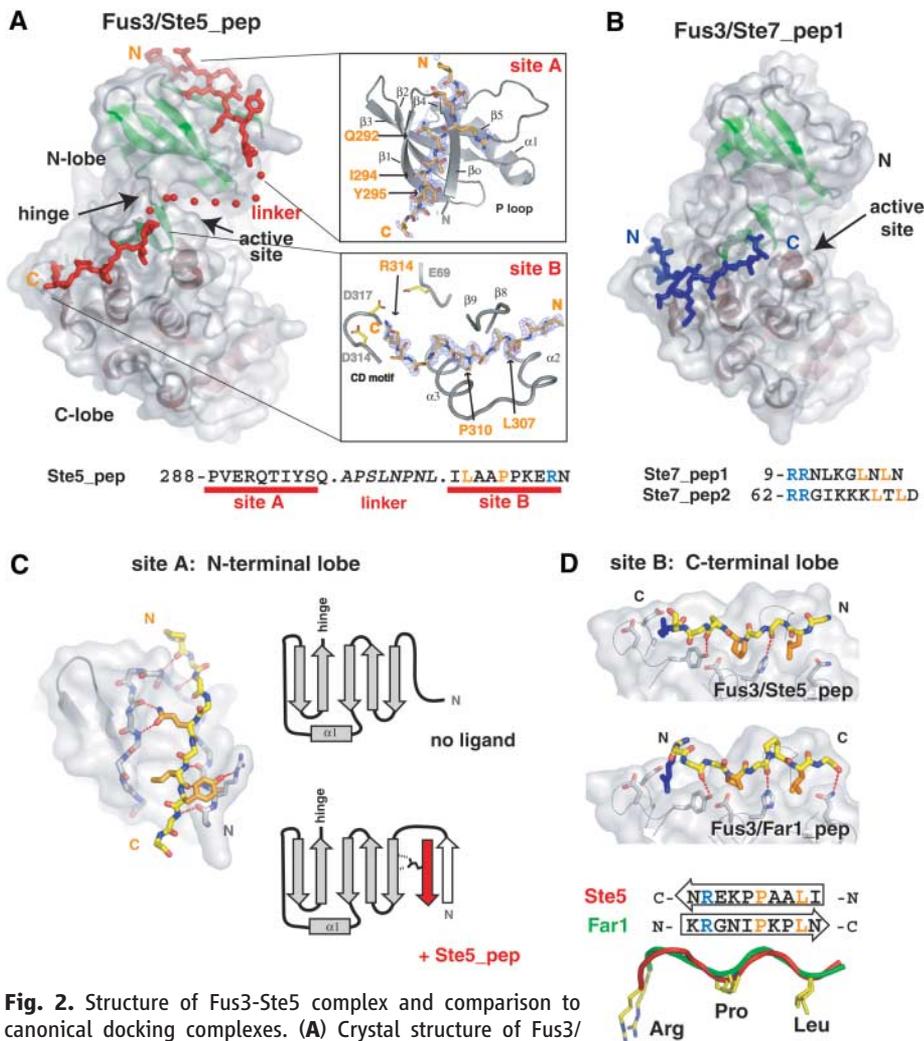
Fig. 2. Structure of Fus3-Ste5 complex and comparison to canonical docking complexes. (**A**) Crystal structure of Fus3/Ste5_pep complex. Ste5 (red) binds to Fus3 in a bipartite manner. Close-up views of site A and site B on the right are shown with simulated annealed electron density omit maps (contoured at 1σ) for the Ste5 peptide. (**B**) Structure of Fus3 in complex with a canonical docking motif from Ste7 (Ste7_pep1) (16). (**C**) Protein-protein interactions at site A. The N-terminal half of Ste5_pep adopts a β-strand conformation and initiates the formation of a new β strand at the N terminus of Fus3 (β0). This strand forms eight backbone-backbone H bonds with the Fus3 N-terminal region (H bonds are indicated with red dashed lines). The side chain of Q^{292} is H bonded to the backbone of β1, the hydrophobic side chain of I^{294} interacts with a groove on the top of the kinase, and Y^{295} makes an H bond with the side chain of R^4 from Fus3. Schematic illustration of secondary structural elements of the N-terminal kinase lobe in the unliganded and Ste5_pep liganded complex is shown on the right. (**D**) Comparison of protein-protein interactions at the canonical MAPK docking groove (site B) between the Fus3/Ste5_pep and the Fus3/Far1_pep complexes (16).

a recently solved complex of Fus3 with a docking peptide from the substrate Far1 (16). Although the peptides bind in opposite orientations, both insert a proline into a central pocket in the Fus3 surface and present a peripheral Arg that forms electrostatic interactions with a conserved pair of Asp residues (Fig. 2D). The backbone trace of these two peptides, although reversed, is virtually identical, as are many of the hydrogen bonds made to the peptide backbone. The flexibility of the Fus3 binding site to recognize peptides in two orientations is reminiscent of the properties of Src homology 3 (SH3) domains and other domains that recognize proline-rich peptides in two possible orientations. In the case of Fus3, both the Far1 and Ste5 peptides, in their central regions, adopt a polyproline II (PPII) helical conformation. PPII helices are twofold rotationally pseudosymmetric; thus, any protein designed to bind this structure will inherently have some ability to recognize peptides in a reverse orientation (20). This recognition flexibility of the MAPK docking groove indicates that there may be additional classes of MAPK interacting motifs that have not yet been identified.

The interactions at the A site have no obvious similarity to previously characterized kinase-peptide interactions. This region of the kinase N-terminal lobe normally forms a five-stranded β sheet. However, upon binding, the Ste5 peptide itself forms a β strand and induces Fus3 residues 5 to 10 to form a sixth β strand, and the region adopts a seven-stranded structure in the form of a β sandwich (Fig. 2C).

Ste5 allosterically activates Fus3 autophosphorylation. The Ste5 fragment not only binds Fus3 in a noncanonical manner but also allosterically stimulates the rate of Fus3 autophosphorylation by ∼50-fold (Fig. 3A). Such strong activation is not observed with any other known Fus3 binding peptides, including the docking motifs from Ste7 (Fig. 3B). Mass spectrometric and mutational analysis indicates that Ste5 stimulation produces a monophosphorylated form of the kinase: Autophosphorylation occurs selectively on Tyr^{182}, one of two residues (Thr^{180} and Tyr^{182}) in the Fus3 activation loop that are normally phosphorylated upon full activation of the MAPK (fig. S3) (21). Monophosphorylation (pTyr) substantially increases kinase activity; with the myelin basic protein as a model MAPK substrate, the ratio of activity of the nonphosphorylated, tyrosine-phosphorylated, and doubly phosphorylated forms of Fus3 is 1:25:120 (fig. S4). Thus, unlike other MAP kinases, such as Erk2 (22), the monophosphorylated form of Fus3 is active in vitro, though it is still activated another four- to fivefold when doubly phosphorylated.

two distinct surfaces. The N-terminal portion of the Ste5 fragment contacts the N-terminal lobe of the kinase (site A), and the C-terminal portion contacts the C-terminal lobe of the kinase (site B). The intervening linker region of eight residues between site A and site B binding motifs is disordered and not visible within the crystal structure. Binding of Ste5_pep buries ∼1000 Å² of surface area with a roughly even contribution from the A and B sites. Neither the A nor the B site fragment from Ste5 independently shows measurable binding to Fus3 (18).

The B site interaction in the Ste5-Fus3 complex overlaps with the binding surface of the kinase that interacts with canonical docking motifs, such as those found in Ste7. This explains why interaction of Fus3 with Ste7 and Ste5 is competitive (19) (Fig. 2, A and B). The nature of the interaction, however, is quite different; the Ste5 fragment lies in the docking groove in an N- to C-terminal orientation that is precisely the opposite of that of the canonical docking peptides. Despite this difference in orientation, the B site interaction bears some similarities to canonical docking interactions, particularly

We solved the structure of the pTyr form of Fus3 (fig. S5). Comparison with the nonphosphorylated form of the kinase provides a model for why the pTyr form shows relatively high activity. Before phosphorylation, part of the activation loop occludes the active site, acting as a pseudo-substrate (16). However, in the pTyr form, the entire activation loop is disordered and no longer blocks substrate accessibility, which likely accounts for the increased kinase activity. The role of the second phosphorylation (pThr) cannot be directly inferred from available Fus3 structures. However, phosphorylation on Thr[180] may stabilize a new conformation of the dislodged activation loop by promoting new interactions with the rest of the kinase, as is observed for the structurally similar mammalian MAPK Erk2 (23).

The allosteric activation of Fus3 by Ste5 is reminiscent of the enhanced autoactivation of mammalian p38α induced by transforming growth factor β–activated protein kinase 1–binding protein 1 (TAB1) (24), although this event leads to dual phosphorylation of p38α rather than monophosphorylation observed for Fus3. Little is known about the mechanistic basis for TAB1-enhanced p38α autophosphorylation.

Mechanism of allosteric activation. How, mechanistically, might the Ste5 polypeptide induce autophosphorylation, and therefore activation, of Fus3? Several pieces of evidence support a model in which the linkage between sites A and B of the Ste5-Fus3 interaction is critical for activation. First, an alignment of peptide-bound and unbound structures observed within the same crystal form (Fig. 3C) reveals that Ste5 binding to Fus3 results in a perturbation of the relative orientation of the N- and C-terminal lobes of the kinase upon Ste5 binding. If such an interdomain hinge motion is important for Fus3 activation, then altering the length of the linker between the site A and site B binding motifs might influence autoactivation. Indeed, lengthening or shortening this linker region by one, two, or three residues reduced the ability of Ste5_pep to enhance Fus3 auto-activation without affecting binding affinity for the kinase (Fig. 3D and fig. S6). Thus, we propose a model in which the Ste5 polypeptide binds to both domains of Fus3, inducing a subtle hinge-bending shift. The shift between the kinase domains may increase the flexibility of the activation loop (25), allowing the Tyr side chain to enter the active site, where it can be autophosphorylated (the rate of autophosphorylation is independent of enzyme concentration, consistent with an intramolecular reaction) (18).

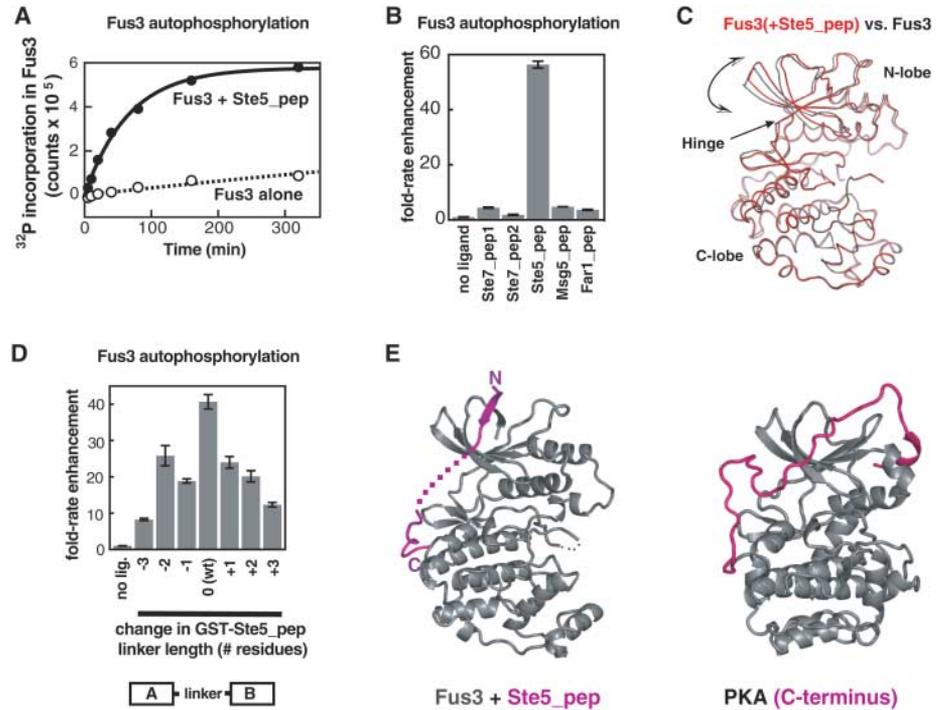The overall topology with which the Ste5 peptide interacts with Fus3 is somewhat

similar to the way in which the C-terminal extension of protein kinase A (PKA) packs against the main kinase domain (Fig. 3E) (26). This C-terminal extension is thought to have an important role in placing the PKA catalytic domain in a constitutively active conformation, perhaps by orienting the two lobes of the kinase in the correct juxtaposition for catalysis (27). In both cases, peptide elements, either inter- or intramolecular, that properly position the two kinase lobes with respect to one another may play an important role in activation.

In vivo analysis: Ste7 docking sites are redundant but essential for pathway signaling. We biochemically characterized three binding sites for Fus3 within the mating signaling complex. To determine the physiological role of these recruitment sites in the mating response, we made mutant alleles of Ste7 (16) or Ste5 in which each of these MAPK recruitment sites was disrupted [nondocking (ND) mutations include disruption of Ste7 docking sites *STE7^ND1^*, *STE7^ND2^*, and *STE7^ND1,2^* and disruption of Ste5 docking

site *STE5^ND^*), and we quantitatively measured their ability to replace the wild-type gene in vivo (Fig. 4). Mating response to increasing α factor was measured by a mating reporter gene [Fus1–green fluorescent protein (GFP)]. Average pathway output per cell was quantitated by flow cytometry (17).

Mutation of either individual Ste7 docking motif reduced maximal pathway output, though output was still clearly detectable (Fig. 4A). However, if both sites were simultaneously mutated (*STE7^ND1,2^*), no pathway output was observed. Similar results were observed by assaying Fus3 phosphorylation and quantitative mating efficiency (18). The effect of disrupting both Ste7 docking peptides is similar to that of disrupting the Ste5-Ste7 interaction (28) and approaches that of deleting Ste7. Hence, it appears that the Fus3 docking sites in Ste7 are essential for pathway signaling, although they are functionally redundant.

In vivo analysis: Allosteric activation site in Ste5 down-regulates pathway output. We expected that the region of Ste5 that bound

Fig. 3. Ste5 allosterically activates Fus3 autophosphorylation. (**A**) Ste5_pep enhances Fus3 autophosphorylation. Fus3 was incubated with no ligand (open circles) or Ste5_pep (closed circles), and data from autoradiograms were fit to an equation describing unimolecular autophosphorylation kinetics. (**B**) No other Fus3 binding peptides strongly promote autophosphorylation. Autophosphorylation rate enhancements (relative to Fus3 activity alone) are plotted. Msg5 is a phosphatase that acts on Fus3, and Far1 is a Fus3 substrate (16). Error bars show 1 SD from a kinetic fit of data averaged from three experiments. (**C**) Comparison of Fus3 with and without Ste5_pep in the same crystal form. (**D**) Effect of lengthening or shortening the linker between the two regions by which Ste5_pep contacts Fus3 (sequence deletions or insertions are listed in table S1). Rate enhancement factors were obtained by measuring [32P] incorporation into Fus3 in the presence of each glutathione S-transferase (GST)–peptide compared with that with GST alone (fig. S6). Error bars show 1 SD derived from a kinetic fit of data from a typical experiment. (**E**) Comparison of Ste5_pep in complex with Fus3 (left) and the C-terminal tail (amino acids 301 to 350) of the catalytic subunit of PKA (right) (26).
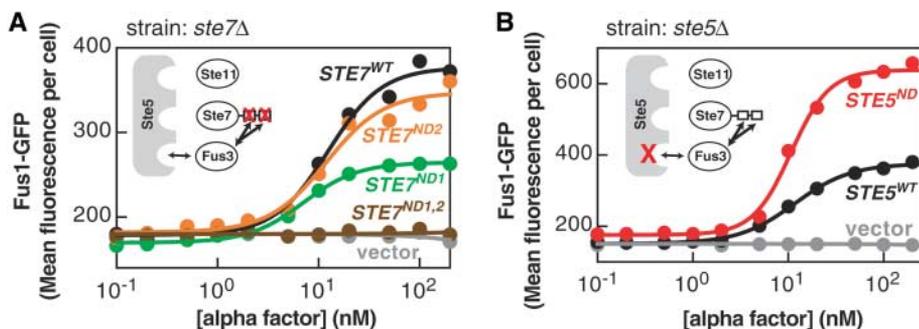
Fig. 4. Negative effects of the Ste5 Fus3 binding region on transcriptional mating response. (**A**) Effects of mutating Ste7 Fus3 interaction sites on the transcriptional mating pathway–dependent reporter Fus1-GFP. Multiple mutations were made in key basic and hydrophobic residues in Ste7_pep1 (allele *STE7ND1*) or Ste7_pep2 (allele *STE7ND2*) to fully disrupt Fus3 binding. GFP expression driven by the pheromone-inducible Fus1 promoter was measured by flow cytometry in yeast expressing the indicated allele of *STE7* in a ste7Δ strain (gray, empty vector; black, *STE7WT*; green, *STE7ND1*; orange, *STE7ND2*; brown, *STE7ND1,ND2*). (**B**) Effect of mutating the Fus3 interaction site on Ste5 on expression of the Fus1-GFP reporter. Multiple mutations were made in key residues of Ste5_pep (allele *STE5ND*) to fully disrupt Fus3 binding (fig. S8; mutations are listed in table S1). Experiments were done in yeast expressing the indicated allele of *STE5* in a ste5Δ strain (gray, empty vector; black, *STE5WT*; red, *STE5ND*). See fig. S7 for histograms from flow cytometry studies.

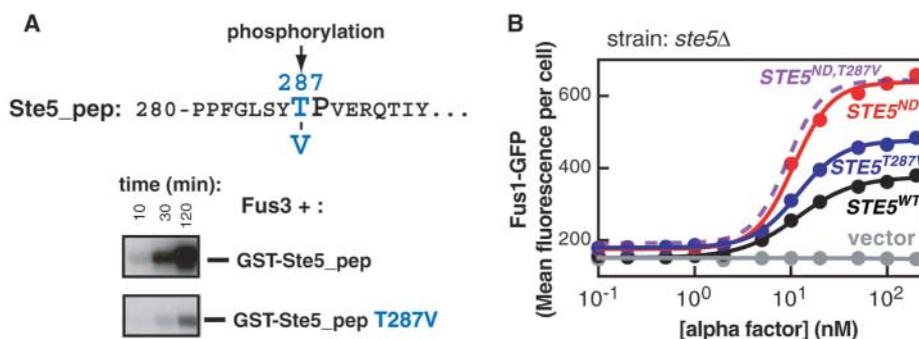**Fig. 5.** Importance of phosphorylation of Ste5 in controlling amplitude of pathway output. (**A**) Phosphorylation by Fus3 of an extended version of the Ste5_pep peptide (amino acids 280 to 321) in vitro. Consensus MAPK phosphorylation sequence (S/T-P) is shown in large type, with putative phosphoacceptor Thr287 shown in blue. Lower panel shows autoradiogram of ^{32}P incorporation into GST fusions of either the extended Ste5_pep or a T287V mutant of the extended peptide, after incubation with Fus3. (**B**) Effect of mutating this phosphoacceptor residue in Ste5 on expression of the Fus1-GFP reporter. The mutation was made in an otherwise wild-type context (allele *STE5T287V*) or in a nondocking allele of Ste5 (allele *STE5ND,T287V*). GFP expression was measured by flow cytometry in yeast expressing the indicated allele of *STE5* in a ste5Δ strain (gray, empty vector; black, *STE5WT*; red, *STE5ND*; blue, *STE5T287V*; fit shown in dashed purple line, *STE5ND,T287V*; data points omitted for clarity).

Fus3 would also make an important contribution to increasing pathway output. Surprisingly, we observed the opposite effect (Fig. 4B and fig. S7). We disrupted the Ste5-Fus3 interaction by mutating six residues distributed through the site A and site B interaction motifs to Ala. [We confirmed that these mutations yield a fragment that can neither bind nor activate Fus3 (fig. S8).] When we replaced wild-type Ste5 with this nonbinding mutant in vivo, we observed a twofold increase in maximal pathway transcriptional output (Fus1-GFP expression). This increase in output level is greater than that which has been observed with most

gain-of-function mutants, such as overexpression or constitutive alleles of pathway members (*29–31*). The transcriptional difference observed with this Ste5 allele is dependent on Fus3, consistent with our observation that the semi-redundant filamentation MAPK, Kss1, does not bind this fragment (*18*). This mutant phenotype suggests that the normal role of the Fus3-binding region in Ste5, with its unusual ability to enhance Fus3 autophosphorylation, is actually to attenuate pathway output.

Thus, contrary to previous simple models, this particular scaffold-MAPK recruitment interaction appears not to promote signaling;

rather, it appears to down-regulate pathway output. In contrast, the MAPKK-MAPK interaction, though redundant, is essential for signaling.
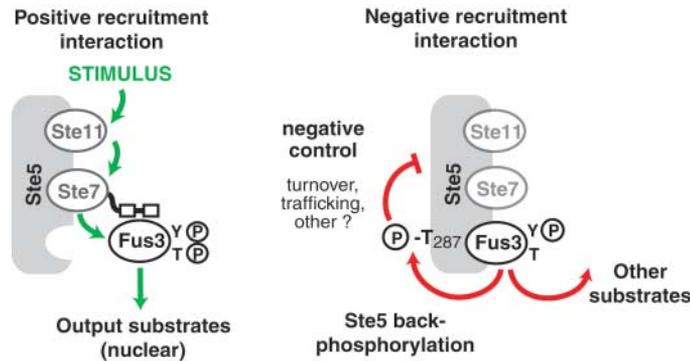
Monophosphorylated Fus3 phosphorylates Ste5 as part of the down-regulatory response. When Ste5 was used to stimulate autophosphorylation of Fus3 in vitro, we noticed that the Ste5 fragment itself became strongly phosphorylated. The Fus3 binding region of Ste5 contains one potential MAPK phosphorylation site (Thr287-Pro288) (Fig. 5A). The Ste5 polypeptide phosphorylation is greatly reduced when this site is mutated [Thr287→Val (T287V)], indicating that this is the primary phosphoacceptor in vitro. Neither phosphorylation of this site nor mutation to Val affects the ability of the polypeptide to bind to and stimulate autoactivation of Fus3 (fig. S9).

Nonetheless, we hypothesized that this phosphorylation of Ste5 might affect pathway down-regulation in vivo, particularly given that feedback phosphorylation occurs elsewhere in the mating pathway (*32–34*) and other MAPK pathways (*35*). To test this model, we examined the effect of replacing wild-type Ste5 with a version bearing the T287V mutation (Fig. 5B). This mutant exhibits increased Fus1-GFP output, partially phenocopying the *STE5ND* mutant that prevents Fus3 binding and auto-activation. The *STE5ND* mutation was also epistatic to the *STE5T287V* mutation; although both mutations individually increased pathway output, a version of Ste5 bearing both mutations showed the same maximal transcriptional output as that observed with the *STE5ND* allele. These findings are consistent with a model in which the mutations affect different steps within the same pathway. Thus, we propose that Fus3, when autoactivated by this fragment of Ste5, may promote increased phosphorylation of Ste5 on Thr287.

The precise mechanism by which autoactivation and consequent scaffold phosphorylation down-regulates pathway transcriptional output remains unclear. Phosphorylation of Ste5 might alter turnover and lower steady-state abundance of Ste5 through degradation; it might alter the trafficking properties of Ste5 (*31, 36*); or this Ste5 phosphorylation event might exert its effects through multiple composite actions. Monophosphorylated Fus3 may also have substrates besides Ste5 that contribute to pathway down-regulation, because the *STE5T287V* allele only partially phenocopies the *STE5ND* allele. The monophosphorylated form of Fus3 may act on distinct substrates from those modified by the dual-phosphorylated, fully active form of the kinase. Alternatively, the mono- and dual-phosphorylated forms of Fus3 might be differentially localized.

Fig. 6. Schematic of the distinct roles for Fus3 binding peptides in the MAPKK Ste7 and the scaffold Ste5. (**Left**) Two redundant peptides in the MAPKK Ste7 that recruit Fus3 are essential for signaling through the pheromone response MAPK pathway. (**Right**) The Fus3 binding site in the Ste5 scaffold limits signal propagation through the MAPK pathway. Recruitment of Fus3 to this site enhances autophosphorylation on Tyr^{182} of Fus3, which may promote Fus3 phosphorylation of other substrates, including Thr^{287} of Ste5. The net effect of these phosphorylation events appears to be a decrease in transcriptional output of the pheromone response MAPK pathway.

Conclusions: Ste5 scaffold shapes quantitative pathway output. We characterized multiple distinct modes of recruitment of the MAPK Fus3 to the yeast pheromone response pathway signaling complex, a prototypical scaffolded MAPK cascade (Fig. 6). The interaction of the MAPK with the MAPKK Ste7 is required for efficient signal propagation. In contrast, the interaction of the MAPK with the scaffold appears to control pathway gain by down-regulating overall output. Thus, the Ste5 scaffold not only functions as an interaction assembly point for the pathway components, but it also serves as a regulatory node that actively participates in tuning pathway flux.

These findings force us to revise models for how Ste5 and its interactions contribute to pathway function, but they do not contradict the fundamental concept that assembly of the MAPK pathway components into a single complex is important for determining the basic wiring of the pathway. Recruitment of Fus3 to the complex is clearly essential for proper signaling, although this recruitment is primarily mediated through interactions with the upstream MAPKK Ste7. Recruitment of other cascade members (MAPKKK Ste11 and MAPKK Ste7) to Ste5 is also essential for signaling (*28*, *37*). However, the Ste5-Fus3 recruitment interaction studied here, which was previously thought to be essential for signaling, actually limits transcriptional pathway output at a systems level. These findings suggest that multiple molecules of Fus3, some playing positive and others playing negative roles, may be part of an individual signaling assembly.

A model in which Fus3 has both positive and negative regulatory roles is reminiscent of the behavior of transcriptional regulators. Promoters, like scaffolds, organize the assembly of transcription factor complexes that determine the degree of gene expression. There are growing examples in which the same transcription factor can play either positive or negative regulatory roles, depending on the exact context of promoter sequence and other cofactors (*38*, *39*).

This work presents evidence of a more complex role for the scaffold Ste5 in regulating the yeast pheromone response pathway. Rather than merely recruiting catalytic components, the scaffold alters the catalytic activity of at least one bound kinase and takes part in a negative regulatory loop that appears to decrease output from the pathway. Other scaffolds may also have multiple roles in shaping signaling responses, including wiring together specific sets of signaling components and controlling and coordinating their behavior to precisely tune the amplitude and dynamics of the response.

References and Notes

1. W. R. Burack, A. S. Shaw, *Curr. Opin. Cell Biol.* **12**, 211 (2000).
2. D. K. Morrison, R. J. Davis, *Annu. Rev. Cell Dev. Biol.* **19**, 91 (2003).
3. E. A. Elion, *J. Cell Sci.* **114**, 3967 (2001).
4. K. Y. Choi, B. Satterberg, D. M. Lyons, E. A. Elion, *Cell* **78**, 499 (1994).
5. S. Marcus, A. Polverino, M. Barr, M. Wigler, *Proc. Natl. Acad. Sci. U.S.A.* **91**, 7762 (1994).
6. J. A. Printen, G. F. Sprague Jr., *Genetics* **138**, 609 (1994).
7. F. Posas, H. Saito, *Science* **276**, 1702 (1997).
8. R. L. Roberts, G. R. Fink, *Genes Dev.* **8**, 2974 (1994).
9. J. E. Ferrell Jr., *Sci. STKE* **2000**, pe1 (2000).
10. M. A. Schwartz, H. D. Madhani, *Annu. Rev. Genet.* **38**, 725 (2004).
11. Single-letter abbreviations for the amino acid residues are as follows: A, Ala; C, Cys; D, Asp; E, Glu; F, Phe; G, Gly; H, His; I, Ile; K, Lys; L, Leu; M, Met; N, Asn; P, Pro; Q, Gln; R, Arg; S, Ser; T, Thr; V, Val; W, Trp; and Y, Tyr.
12. A. J. Bardwell, L. J. Flatauer, K. Matsukuma, J. Thorner, L. Bardwell, *J. Biol. Chem.* **276**, 10374 (2001).
13. C. I. Chang, B. E. Xu, R. Akella, M. H. Cobb, E. J. Goldsmith, *Mol. Cell* **9**, 1241 (2002).
14. T. Lee *et al.*, *Mol. Cell* **14**, 43 (2004).
15. T. Tanoue, M. Adachi, T. Moriguchi, E. Nishida, *Nat. Cell Biol.* **2**, 110 (2000).
16. A. Remenyi, M. C. Good, R. P. Bhattacharyya, W. A. Lim, *Mol. Cell* **20**, 951 (2005).
17. Materials and methods are available as supporting material on *Science* Online.
18. R. P. Bhattacharyya, A. Remenyi, M. C. Good, C. Bashor, W. A. Lim, unpublished data.
19. A. B. Kusari, D. M. Molina, W. Sabbagh Jr., C. S. Lau, L. Bardwell, *J. Cell Biol.* **164**, 267 (2004).
20. A. Zarrinpar, R. P. Bhattacharyya, W. A. Lim, *Sci. STKE* **2003**, re8 (2003).
21. A. Gartner, K. Nasmyth, G. Ammerer, *Genes Dev.* **6**, 1280 (1992).
22. D. J. Robbins *et al.*, *J. Biol. Chem.* **268**, 5097 (1993).
23. B. J. Canagarajah, A. Khokhlatchev, M. H. Cobb, E. J. Goldsmith, *Cell* **90**, 859 (1997).
24. B. Ge *et al.*, *Science* **295**, 1291 (2002).
25. M. Huse, J. Kuriyan, *Cell* **109**, 275 (2002).
26. D. R. Knighton *et al.*, *Science* **253**, 407 (1991).
27. M. Batkin, I. Schvartz, S. Shaltiel, *Biochemistry* **39**, 5366 (2000).
28. S. H. Park, A. Zarrinpar, W. A. Lim, *Science* **299**, 1061 (2003).
29. F. Drogen *et al.*, *Curr. Biol.* **10**, 630 (2000).
30. N. Hao, N. Yildirim, Y. Wang, T. C. Elston, H. G. Dohlman, *J. Biol. Chem.* **278**, 46506 (2003).
31. P. M. Pryciak, F. A. Huntress, *Genes Dev.* **12**, 2684 (1998).
32. B. Errede, Q. Y. Ge, *Philos. Trans. R. Soc. London Ser. B* **351**, 143 (1996).
33. A. Flotho, D. M. Simpson, M. Qi, E. A. Elion, *J. Biol. Chem.* **279**, 47391 (2004).
34. M. V. Metodiev, D. Matheos, M. D. Rose, D. E. Stone, *Science* **296**, 1483 (2002).
35. M. K. Dougherty *et al.*, *Mol. Cell* **17**, 215 (2005).
36. S. K. Mahanty, Y. Wang, F. W. Farley, E. A. Elion, *Cell* **98**, 501 (1999).
37. C. Inouye, N. Dhillon, T. Durfee, P. C. Zambryski, J. Thorner, *Genetics* **147**, 479 (1997).
38. J. A. Lefstin, K. R. Yamamoto, *Nature* **392**, 885 (1998).
39. A. Remenyi, H. R. Scholer, M. Wilmanns, *Nat. Struct. Mol. Biol.* **11**, 812 (2004).
40. L. Bardwell, J. G. Cook, E. C. Chang, B. R. Cairns, J. Thorner, *Mol. Cell. Biol.* **16**, 3637 (1996).
41. We thank J. Weissman, J. Newman, M. Noble, J. DeRisi, and M. Bigos for assistance with flow cytometry; A. Frankel, A. Ramirez, and M. Daugherty for assistance with peptide synthesis; D. King and E. Witkowska for assistance with mass spectrometry; and J. Weissman, D. Morgan, A. Bhatt, S. Collins, V. Denic, J. Dueber, and members of the Lim lab for helpful discussion. This work was supported by a postdoctoral fellowship from the Jane Coffin Childs Memorial Fund for Medical Research (A.R.), the University of California–San Francisco Medical Scientist Training Program and Burroughs Wellcome Fund Program in Quantitative Biology fellowship (R.P.B.), a University of California Graduate Research and Education in Adaptive Bio-Technology fellowship (C.J.B.), and grants from the NIH and Sandler Kirsch Foundations (W.A.L.). Coordinates have been deposited in the Protein Database (2F49, Fus3/Ste5_pep; 2FA2, Fus3 without Ste5_pep; 2F9G, Fus3-pY).